The establishment of the duplex real-time RT-PCR assay for the detection of CD44v6 in pancreatic cancer patients and clinical application

Biotechnology and Applied Biochemistry

*Gang Zhou,[1] David Chiu,[1] Dajiang Qin,[2] Lizhi Niu,[1] Jinlei Cai,[2] Lihua He,[1] Wenhao Huang,[2] and Kecheng Xu[1]**

[1]Department of Oncology, The GIBH Affiliated Fuda Hospital, Chinese Academy of Sciences, Guangzhou, People' s Republic of China

[2]Stem Cell Research Group, Guangzhou Institutes of Biomedicine and Health, Chinese Academy of Sciences, Guangzhou, People' s Republic of China

Abstract.

Cell adhesion molecule *CD44v6* has been found to be associated with the progression and metastasis of numerous cancers. In this study, a novel duplex real-time quantitative reverse-transcription PCR (qRT-PCR) assay was developed to quantitatively detect the *CD44v6* gene expression in pancreatic cancer patients. The primers and probes of *CD44v6* and β*-actin* genes were designed and standard curve of the duplex qRT-PCR was constructed by optimizing the reaction conditions. The specificity and reproducibility of this assay were satisfactory and the detection limit was 100 copies, which was 10 times more sensitive than the conventional RT-PCR assay. This assay was also used to detect the expression levels of *CD44v6* messenger RNA in peripheral blood mononuclear cell in 37 pancreatic cancer patients and 12 healthy people. The results showed that 37 clinical samples were tested positive by the duplex qRT-PCR compared with only 30 by the conventional RT-PCR. The levels of *CD44v6* expression showed significant correlation with sex, tumor size, tumor differentiation, clinical stage, lymph node, and liver metastasis ($P < 0.05$). Compared with the control group, *CD44v6* levels in patients prior and 10 days post cryosurgery were significantly increased ($P < 0.05$) but had no significant change in those 1 month post cryosurgery ($P > 0.05$). The duplex qRT-PCR assay may provide a useful tool for the evaluation of prognosis and curative effect of pancreatic cancer.

Volume 00, Number 0, Pages 1–9 •
E-mail: xukc@vip.163.com

Keywords: *CD44v6*, quantitative real-time RT-PCR, pancreatic cancer

1. Introduction

Pancreatic cancer is one of the most lethal human cancers because of its rapid growth and propensity to invade adjacent organs [1]. Because of the lack of significant symptoms, patients cannot be diagnosed immediately and less than 20% of the patients are candidates for surgical resection. The survival rate of the pancreatic cancer patients in 5 years is less than 5% [2]. However, if this disease were diagnosed at an early stage, nearly 25%–30% of the patients have shown a 5-year survival period post surgery [3]. Thus, the identification of biological markers that could provide prognostic information about the invasive or metastatic potential of pancreatic cancer becomes essential for the diagnosis and treatment of this disease.

The cell adhesion molecules, including integrins, cadherins, immunoglobulins, and *CD44s*, are essential for cell–cell and cell–extracellular matrix interactions [4],[5]. More importantly, the cell adhesion molecules are involved in cellular proliferation, migration, and differentiation. The distribution of *CD44* is very extensive and can be detected in lymphocytes and fibroblasts [6]. At least 20 variants (v) of CD44 have been reported by the alternative splicing of 10 extrons (v1–v10) that encode the proximal portion of the extracellular domain [7]. The expression of *CD44v6 (v6)*, which is closely related to the progression, metastasis, and prognosis of a tumor, has been studied in several malignant neoplasms [8–11]. However, the lack of absolute quantitative detection methods, which can test the expression levels of *CD44v6* exactly within the cells or tissues, has limited the potential application of *CD44v6* as a biomarker.

As no studies thus far have examined the expression levels of *CD44v6* mRNA quantitatively in pancreatic cancer patients, a duplex quantitative reverse-transcription PCR (qRT-PCR) method to quantify the copy number of *CD44v6* mRNA accurately in peripheral blood mononuclear cells (PBMCs) of

Abbreviations: qRT-PCR, quantitative reverse-transcription PCR; PBMCs, peripheral blood mononuclear cells; TNM, Tumor Node Metastasis; Ct, cycle threshold; HS-ExTaq, Hotstart ExTaq polymerase; CV, coefficient variation; SD, standard deviation; EDTA, ethylenediaminetetraacetic acid; TE, Tris-EDTA; DNase, deoxyribonuclease; Rnase, ribonuclease; ELISA, enzyme-linked immunosorbent assay.

*Address for correspondence: Kecheng Xu, PhD, Department of Oncology, The GIBH Affiliated Fuda Hospital, Chinese Academy of Sciences, 91 Ju de Zhong Road, Chigang, Guangzhou, People's Republic of China. Tel: +86-20-34471287; Fax: +86-20-34471288; e-mail: xukc@vip.163.com.

Received 23 June 2011; accepted 6 December 2011
DOI: 10.1002/bab.69
Published online in Wiley Online Library (wileyonlinelibrary.com)

Table 1
Primers and TaqMan fluorogenic probes used in this research

Gene	Name	Sequence(5′-3′)	GenBank	Length
	C-F	CCAGGCAACTCCTAGTAGTACAAC		
CD44v6	C-R	GGGAGTCTTCTCTGGGTGTTTG	L05415	107 bp
	C[a]	TGCCATCTGTTGCCAAACCACTGTTCCT		
	β-F	CGGGACCTGACTGACTACCTC		
β-actin	β-R	CCATCTCTTGCTCGAAGTCCAG	M10277	136 bp
	β[b]	TCCTTAATGTCACGCACGATTTCCCGCT		

[a]The probe of *CD44v6* gene was labeled with 5′-6-carboxy-fluorescein (FAM) and 3′-6-carboxytetramethyl-rhodamine (TAMRA).

[b]The probe of *β-actin* gene was labeled with 5′-6-carboxy-X-rhodamine (ROX) and 3′-Black Hole Quencher 2 (BHQ2).

37 pancreatic cancer patients was established in this study. The new method could offer great benefits in the diagnosis of pancreatic cancer using *CD44v6* as a biomarker, the study of the relationship between the expression of *CD44v6* and the invasion, infiltration, and metastasis of pancreatic cancer, and the evaluation of therapy effectiveness in pancreatic cancer patients.

2. Materials and methods

2.1. Patients and PBMCs

Thirty-seven pancreatic cancer patients were enrolled in Fuda Hospital in Guangzhou, People's Republic of China, including 22 males and 15 females, at an average age of 58 ± 15.3 years. In total, 22 heads, five bodies, and 10 tails of pancreatic cancer were diagnosed by pathology. According to the standard of Tumor Node Metastasis (TNM), only one patient belonged to I stage and five, seven, and 24 patients belonged to II, III, and IV stages, respectively. Only 18 of the total 37 patients had performed argon–helium cryosurgery. Twelve healthy people in Fuda Hospital were selected randomly as normal controls and no tumor history was found among them; included were seven males and five females, at an average age of 47 ± 14.2 years.

About 3 mL ethylenediaminetetraacetic acid (EDTA) anticoagulation was collected from healthy people as well as the patients prior cryosurgery, 10 days, and 1 month post cryosurgery, respectively. PBMCs were isolated by the Ficoll-Paque Plus (Invitrogen, Shanghai, People's Republic of China) according to the manufacturer's protocol.

2.2. Total RNA extraction and cDNA synthesis

Total RNA was extracted from each PBMC immediately with an RNA isolation plus according to the manufacturer's instructions (TaKaRa, Dalian, People's Republic of China). RNA samples were resuspended in diethypyrocarbonate-treated water (TaKaRa). The quality of RNA samples was confirmed by formaldehyde gel electrophoresis. All RNA samples were treated with deoxyribonuclease (DNase) I (TaKaRa) prior to reverse transcription to avoid the contamination of the genome DNA. The absence of contaminated genomic DNA in the RNA samples was verified by running PCR directly without reverse transcription.

The cDNA synthesis was performed in a 20 μL reaction volume containing 1 μg total RNA, 1 × RT-PCR buffer, 1 mM dNTPs, 0.75 μM oligo dT, 2 U of ribonuclease (Rnase) inhibitor, and 2.5 U of M-MLV reverse transcriptase (TaKaRa) at 42°C for 1 H according to the manufacturer's instructions. The cDNA was five times diluted using Dnase- and Rnase-free molecular-biology grade water (TaKaRa) and 2 μL of the diluted cDNA was used for each amplification reaction.

2.3. Primers and probes for the duplex qRT-PCR

The human *CD44v6* gene sequences were retrieved from the GenBank database (GenBank ID: XM002821884, AB468969, BC004372, L05415, X62739, AJ251595, NG008937, XM001115359, and U46958) and aligned using the DNAStar program. Only a highly conserved region was used to design the primers and TaqMan probe using Beacon Designer software version 7.0 (Palo Alto, CA, USA). BLAST search was conducted to confirm the specificity of the nucleotide sequences chosen for the design of the primers and probe. The sequences of primers and probe of *β-actin* gene were designed based on a conserved region of human *β-actin* gene (GenBank ID: NG022872, XM096887, XM096458, XM096372, XM096268, XM092509, and M10277). The optimal primers and probes (Table 1) were synthesized by Invitrogen.

2.4. Preparation of standard plasmids for the duplex qRT-PCR

The conventional RT-PCR amplifications of *CD44v6* and *β-actin* genes from PBMC cDNA were performed, respectively, with the primers in Table 1. The PCR products were cloned into pMD18-T vector (TaKaRa) according to the manufacturer's instructions. Plasmid DNA from recombinant clones was extracted using a plasmid isolation kit (Biowatson, Shanghai, People's Republic of China), according to the manufacturer's protocol and sequenced by Invitrogen. The concentration of *CD44v6* and *β-actin* plasmid DNA was measured with an ultraviolet spectrophotometer (Eppendorf, Hamburg, Germany) and the copy

number was calculated according to the following equation:

$$\text{Copy number (copies}/\mu\text{L)} = \frac{\text{NA (copies/mol)} \times \text{concentration (g}/\mu\text{L)}}{\text{MW(g/mol)}}$$

where NA = Avogadro's number and MW of double DNA = base number × 660.

2.5. The optimization of the duplex qRT-PCR assay

The duplex qRT-PCR was performed in a 25 μL reaction system using the ABI PRISM 7300 Real-time PCR system (Applied Biosystems, CA, USA). Various PCR parameters such as annealing temperatures from 55°C to 62°C, primer concentration from 0.2 to 0.8 μM, and of probes from 0.1 to 0.5 μM were optimized. Optimal conditions showing the highest fluorescent signal and the lowest cycle threshold (C_t) were selected.

Finally, the optimal duplex qRT-PCR reaction system contained 2.5 μL of 10 × buffer, 2 μL of 2.5 mM dNTPs, 0.5 μL of 10 μM C-F primer, 0.5 μL of 10 μμ C-R primer, 0.25 μL of FAM-labeled *CD44v6* probe, 0.5 μL of 10 μM β-R primer, 0.5 μL of 10 μM β-F primer, 0.25 μL of ROX-labeled *β-actin* probe, 0.4 μL of 5 U Hotstart ExTaq polymerase (HS-ExTaq) (TaKaRa), 1 μL template DNA, and 15.35 μL distilled water. The optimal reaction process was as follows: 94°C for 3 Min followed by 40 cycles of 94°C for 15 Sec and 61°C for 45 Sec.

2.6. The construction of the standard curves for the duplex qRT-PCR assay

The recombinant plasmids (10^{10} copies/μL) of *CD44v6* and *β-actin* genes were diluted 10-fold serially using Tris-EDTA (TE) buffer. To construct the standard curves of the duplex qRT-PCR assay, serial dilutions from 10^3 to 10^9 copies/μL of the *CD44v6* and *β-actin* plasmid DNA were amplified using this optimized assay (Note: each dilution of these plasmids was amplified in the same tube). The standard curves were produced by plotting the C_t values against the copy number of the serially diluted plasmids.

2.7. Specificity, sensitivity, and reproducibility of the duplex qRT-PCR assay

The specificity of the primer pairs shown in Table 1 was evaluated by the melting curve analysis of SYBR-Green real-time PCR. Both the SYBR-Green real-time PCR assay for *CD44v6* and *β-actin* genes contained 12.5 μL of 2 × SYBR PCR mastermix (TaKaRa), 1 μL of PBMC cDNA, and sterile water to a final volume of 25 μL. The amplification reactions were performed in the ABI PRISM 7300 real-time PCR detection system (Applied Biosystems, USA) following the process described: 3 Min incubation at 95°C followed by 40 cycles of 94°C for 10 Sec and 60°C for 30 Sec. The melting curve was constructed by increasing the temperature from 70°C to 92 °C with a temperature transition rate of 0.4 °C/Sec. All reactions were run in duplicate and sterile water was tested along with the sample as negative control. To ensure that the correct products were amplified in the reaction, all samples were identified by 2% agarose gel electrophoresis.

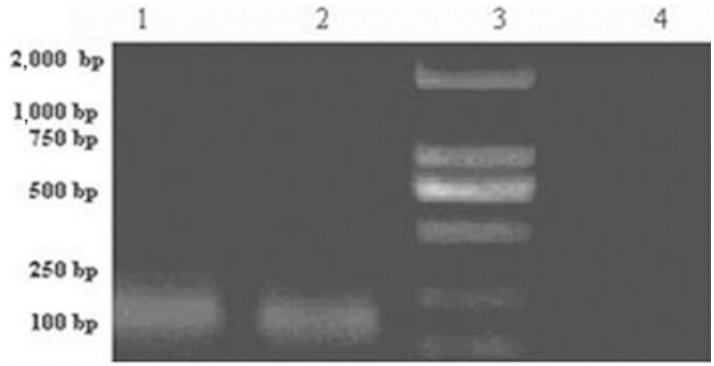

Fig. 1. Agarose gel photograph of *CD44v6* and *β-actin* amplicons amplified from recombinant plasmids using RT-PCR. The *CD44v6* and *β-actin* recombinant plasmids were identified by conventional RT-PCR using specific primers, and specific 107 and 136 bp amplicons were detected from *CD44v6* and *β-actin* recombinant plasmids, respectively (lanes 1 and 2). No band was observed from negative control (lane4); lane 3 was 2,000 bp DNA ladders.

To compare the sensitivity between the triplex qRT-PCR and conventional RT-PCR assay, 10-fold dilutions of the recombinant plasmids were tested employing the two assays. Serial dilutions of the recombinant plasmids ranging from 10^3 to 10^9copies/μL were amplified to assess the reproducibility of the duplex qRT-PCR. Each dilution was repeated four times. Intraassay and interassay variations were determined by calculating the mean C_t values, SD, and coefficient of variation (CV) separately for each plasmid dilution.

2.8. The detection of PBMC samples from pancreatic cancer patients

The serially diluted recombinant plasmids, along with the cDNAs of PBMCs, for detection were tested simultaneously. Then the copy numbers of *CD44v6* and *β-actin* genes in PBMCs were extrapolated from the standard curves of *CD44v6* and *β-actin* genes in each run. Negative control (sterile water) was also performed for each run. For each sample, the copy number of *CD44v6* gene in a million PBMCs was expressed as the number of *CD44v6* copies per 10^6 *β-actin* copies. This calculation method has been used widely in many studies on real-time PCR assay and obtained a satisfactory result [12],[13]. All 37 samples were also checked with the conventional RT-PCR assay using the primers listed in Table 1. All data were shown as mean ± SD and calculated by *t*-test of SPSS 17.0 statistical software. $P < 0.05$ was considered statistically significant.

3. Results

3.1. The identification of *CD44v6* and *β-actin* recombinant plasmids

The special bands from the PCR amplifications of *CD44v6* and *β-actin* recombinant plasmids were observed in Fig. 1. The size of the bands was consistent with the prospective length of

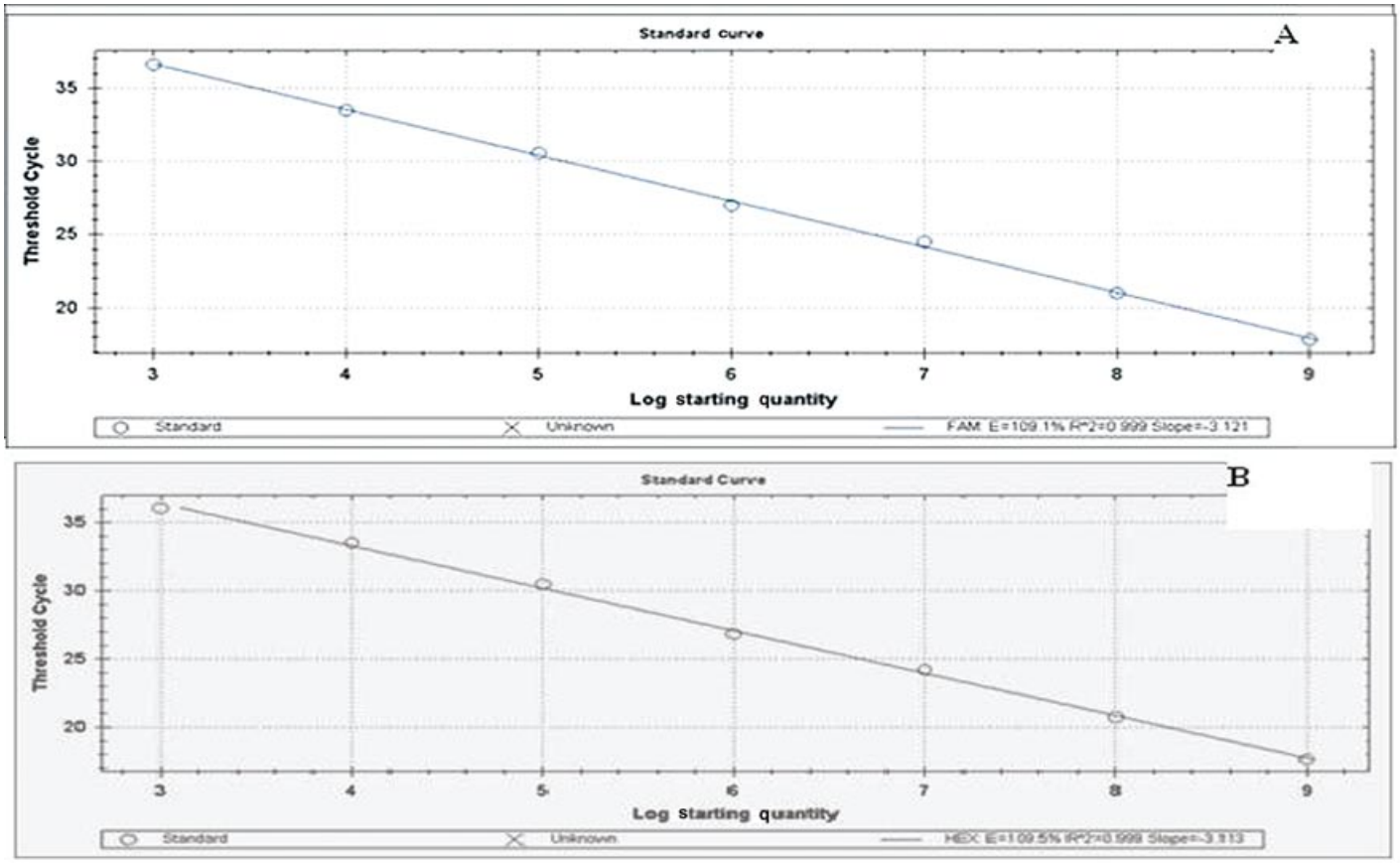

Fig. 2. Duplex qRT-PCR standard curves generated from *CD44v6* and β-*actin* plasmid amplication plots. Standard curves were plotted between copy number of recombinant plasmids and cycle threshold (C_t). (A) *CD44v6* plasmid ranged from 10^3 to 10^9 copies/μL and (B) β-*actin* plasmid ranged from 10^3 to 10^9 copies/μL.

amplicon sizes, which were 107 and 136 bp for *CD44v6* and β-*actin* genes, respectively. The *CD44v6* and β-*actin* gene fragments contained in the respective recombinant plasmids showed 100% homology with the parental sequences, which were used for the primer design (data not shown).

3.2. Standard curves of the duplex qRT-PCR

Detectable fluorescent signals above the threshold were observed at 16.78 and 17.20 cycles for the amplifications of the *CD44v6* and β-*actin* plasmids, respectively (data not shown). Linear standard curves of the *CD44v6* and β-*actin* genes were obtained from 10^3 to 10^9 copies per reaction (Figs. 2A and 2B) with C_t values ranging from 16.78 to 36.72 cycles (R^2: 0.999; reaction efficiencies: 109.1%) and 17.20 to 36.85 cycles (R^2: 0.998; reaction efficiencies: 109.5%), respectively.

3.3. Specificity of the primers used in the duplex qRT-PCR

As shown in Fig. 3A, single and sharply defined melting curves with narrow peaks were obtained for SYBR-Green real-time PCR products of the *CD44v6* and β-*actin* genes at temperature 82°C and 87°C, respectively. The duplicate samples produced almost the same peaks and no fluorescent signal was detected from the negative control. The PCR products were confirmed by 2% agarose gel electrophoresis and specific bands of *CD44v6* and β-*actin* genes were visible, whereas no band was detected from negative control (Fig. 3B).

3.4. Comparison of the sensitivity for the duplex qRT-PCR and conventional RT-PCR assay

The *CD44v6* and β-*actin* recombinant plasmids were diluted serially 10-fold with TE buffer from 10 to 10^9 copies/μL and fluorescent signals were detected from 10^2 to 10^9 copies/μL for *CD44v6* and β-*actin* plasmids by the duplex qRT-PCR assay (Figs. 4A and 4B), whereas the special bands were only detected from 10^3 to 10^9 copies/μL using the conventional RT-PCR assay (Fig. 4C).

3.5. Reproducibility of the duplex qRT-PCR assay

The intra-assay CV of the serial *CD44v6* dilutions ranged from 1.69% to 4.46%, whereas β-*actin* ranged from 1.46% to 4.50%. The CV of the *CD44v6* and β-*actin* dilutions in intra- and inter-assay ranged from 2.67% to 4.80% and 2.56% to 4.68%, respectively (Table 2).

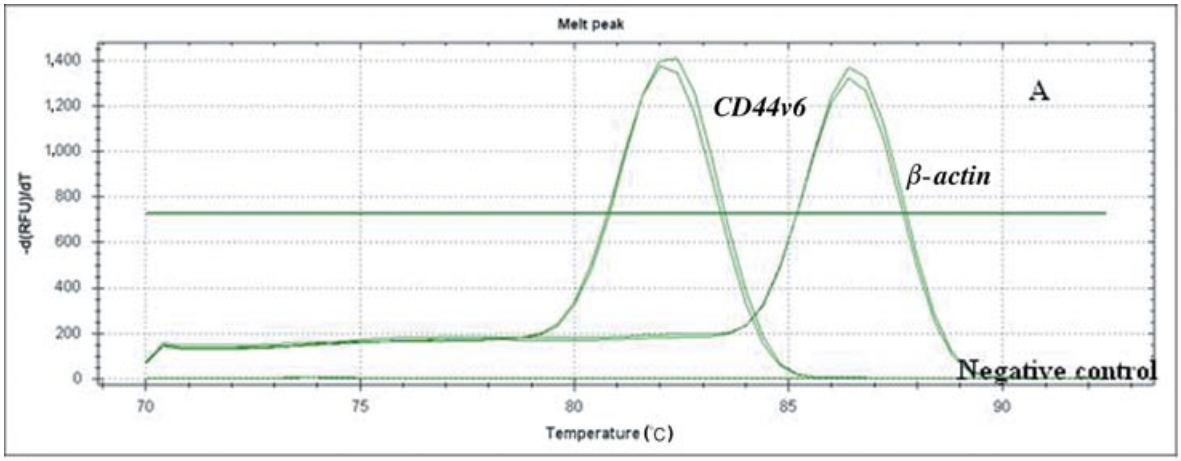

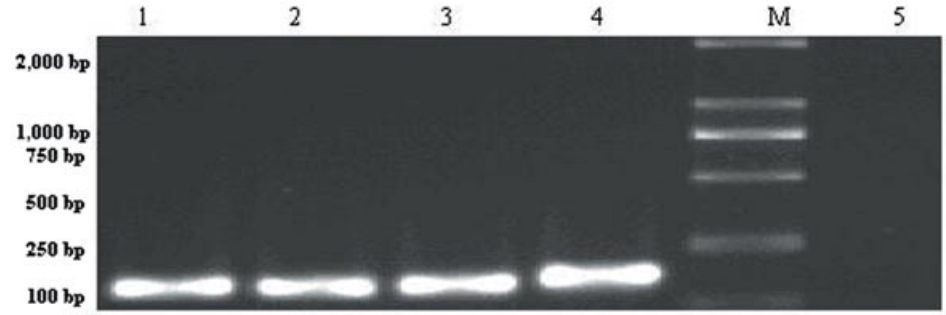

Fig. 3. Melting curve analysis of the SYBR-Green real-time PCR products for *CD44v6* and *β-actin* gene. Only one specific sharp peak was observed for both *CD44v6* and *β-actin* amplification and the duplicate sample produced almost the same peak (A). No band was obtained from negative control (lane 5). The band of 107 bp was obtained from *CD44v6* SYBR-Green real-time PCR products (lanes 1 and 2) and 136 bp was generated from *β-actin* SYBR-Green real-time PCR products (lanes 3 and 4). Lane M was 2,000 bp DNA ladders.

3.6. The detection of PBMC samples from pancreatic cancer patients

A total of 37 samples were collected from preoperative patients and all samples were positive by the duplex qRT-PCR assay, whereas only 30 samples were positive by the conventional qRT-PCR (Table 3). A total of 18 pancreatic cancer patients showed the lower expression levels of *CD44v6* and the log 10 value of *CD44v6* copies per million PBMCs ranged from 3.4 to 3.9, whereas the other 14 patients ranged from 4.0 to 5.0 and only five patients exceeded 5.0 (data not shown).

3.7. The relationship between the expression levels of *CD44v6* mRNA and pathological characteristics of pancreatic cancer

As shown in Table 4, sex, tumor size, and tumor differentiation were significantly associated with the expression levels of *CD44v6* ($P < 0.05$). Age was not significantly related to the levels of *CD44v6* expression ($P > 0.05$). The *CD44v6* levels in body and tail of pancreatic cancer were higher than those in head of pancreatic cancer but no statistically significant difference was found between them ($P > 0.05$). Clinical stage, lymph node, and liver metastasis were all significantly associated with the levels of *CD44v6* expression ($P < 0.05$).

3.8. The expression levels of *CD44v6* in the control group and pancreatic cancer patients prior and post cryotherapy

As shown in Fig. 5, the *CD44v6* expression levels in patients prior and 10 days post cryotherapy are significantly higher than those of the control group ($P < 0.05$). No significant difference was found between the patients 1 month post cryotherapy and control group ($P > 0.05$). Compared with the *CD44v6* levels in patients prior cryotherapy, the *CD44v6* levels in patients 10 days post cryotherapy had no significant change ($P > 0.05$), whereas those in patients 1 month post cryotherapy were significantly decreased ($P < 0.05$). There was no significant difference in the levels of *CD44v6* expression between the patients 10 days and 1 month post cryotherapy ($P > 0.05$).

4. Discussion

Cell adhesion effect was associated with tumor progression, invasion, and metastasis [14],[15]. The modified expression of

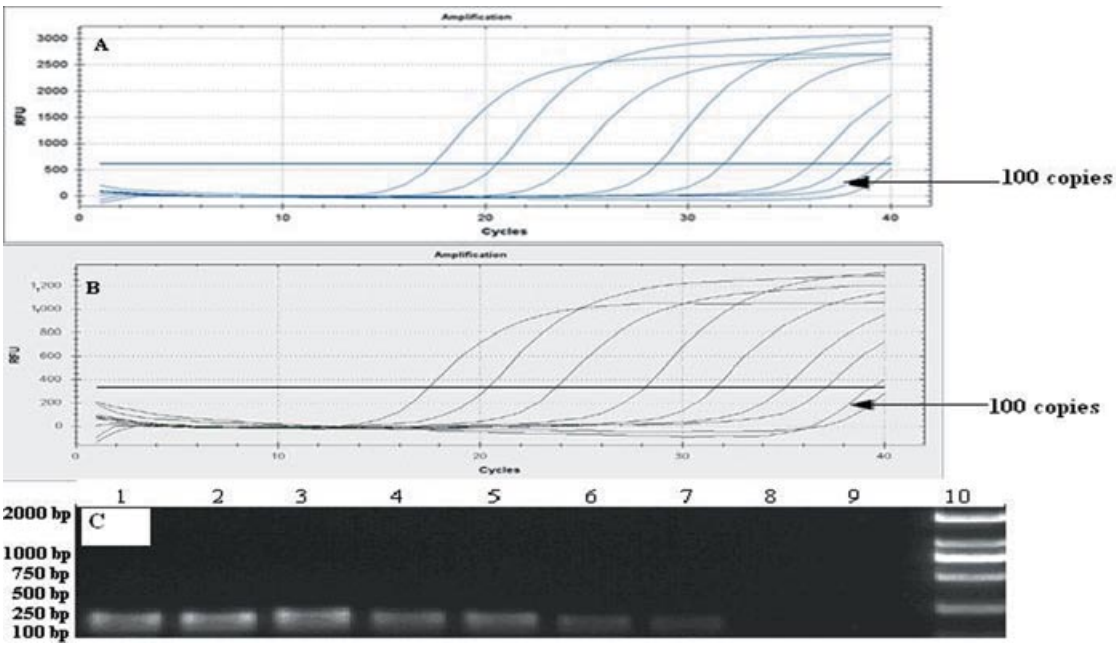

Fig. 4. Sensitivity of the duplex qRT-PCR and conventional RT-PCR assay. Both the *CD44v6* and *β-actin* plasmid DNA were diluted serially 10-fold from 10 to 10^9 copies/μL and detectable fluorescence signals above the threshold were observed from 100 to 10^9 copies/μL for the plasmids (A and B). The detectable bands were produced from 10^3 to 10^9 copies/μL for the *CD44v6* and *β-actin* plasmids (lanes 1–7) and no band was observed from 100 to 10 copies/μL (lanes 8 and 9). (The special bands for CD44v6 and *β-actin* plasmids cannot be separated because the amplicon size of *CD44v6* and *β-actin* gene was almost the same.) Lane 10 was 2,000 bp DNA ladders (C).

Table 2
The reproducibility of the duplex qRT-PCR assay

		Intra-assay						Interassay					
		CD44v6 (C_t)			*β-actin* (C_t)			*CD44v6* (C_t)			*β-actin* (C_t)		
RNA Copy	*n*	Mean	SD	CV%	Mean	SD	CV%	Mean	SD	CV%	Mean	SD	CV%
10^9	4	17.22	0.67	3.89	17.02	0.63	3.70	17.35	0.77	4.44	17.24	0.75	4.35
10^8	4	20.34	0.72	3.54	20.13	0.55	2.73	20.56	0.65	3.16	20.43	0.75	3.67
10^7	4	23.78	0.76	3.20	23.44	0.66	2.82	23.85	0.86	3.61	23.77	0.91	3.83
10^6	4	27.33	1.22	4.46	26.87	1.21	4.50	27.29	1.31	4.80	27.12	1.27	4.68
10^5	4	30.75	0.52	1.69	30.13	0.44	1.46	30.67	0.82	2.67	30.52	0.78	2.56
10^4	4	33.98	0.87	2.56	33.31	0.82	2.46	33.95	1.09	3.21	33.87	1.11	3.28
10^3	4	37.18	0.94	2.53	36.74	0.94	2.56	37.22	1.13	3.04	37.29	1.21	3.24

Table 3
The detection of clinical samples by the duplex qRT-PCR and conventional RT-PCR

Assay	Positive number	Negative number	Total number
Conventional RT-PCR	30	7	37
Duplex RT-PCR	37	0	37

CD44v6 in malignant tumors could affect the cellular adhesion, facilitate the tumor progression, and favor metastasis [16],[17]. Several studies have been carried out to clarify the role of *CD44v6* in different human neoplasms [18–20]. However, so far, there are no studies correlating the mRNA expression of the *CD44v6* gene in pancreatic cancer patients. Therefore, it becomes vitally essential to establish an effective method for the quantitative detection of *CD44v6* gene in pancreatic cancer patients.

In the past several years, immunohistochemisty, RT-PCR, enzyme-linked immunosorbent assay (ELISA), and molecular hybridization assay were used for the detection of *CD44v6* gene [21–23]. However, only the tissue samples can be tested by the immunohistochemistry assay so that surgery is essential for the collection of clinical specimens. The conventional RT-PCR assay cannot quantitatively detect the gene expression level in the tissues or cells. Because ELISA and molecular hybridization assays lack sensitivity, many samples with lower gene expression levels cannot be tested positive.

Table 4
Relation between *CD44v6* mRNA expression levels and pathological features of pancreatic cancer

Pathological features	*N*	Lg value of *CD44v6* mRNA copies per million PBMCs	*P*
Sex			0.037
Male	22	4.65 ± 0.64	
Female	15	4.17 ± 0.69	
Age (years)			0.301
<60	14	4.58 ± 0.64	
>60	23	4.37 ± 0.72	
Tumor position			0.068
Head	22	4.28 ± 0.69	
Body and tail	15	4.70 ± 0.64	
Tumor size (cm)			0.038
<4	15	4.17 ± 0.61	
>4	22	4.64 ± 0.69	
Tumor differentiation			0.047
Low	9	4.10 ± 0.63	
Middle and high	28	4.57 ± 0.68	
Clinical stage			0.039
I–III	13	4.19 ± 0.75	
IV	24	4.60 ± 0.63	
Lymph nodes metastasis			0.035
−	12	4.13 ± 0.55	
+	25	4.61 ± 0.71	
Liver metastasis			0.004
−	14	4.04 ± 0.67	
+	23	4.70 ± 0.59	

Currently, a real-time PCR technique has been developed and used widely for the rapid, sensitive, and accurate detection of gene expression in various cancers [24–26]. Quantification of *CD44v6* gene by the real-time RT-PCR described in this study has several advantages over conventional methods. First, many clinical samples such as tissue, blood, and cells can be tested. Therefore, it is more convenient in the preparation of specimens compared with the immunohistochemistry assay. Second, the qRT-PCR assay not only realized the quantitative analysis of the gene expression but also was more sensitive and specific than

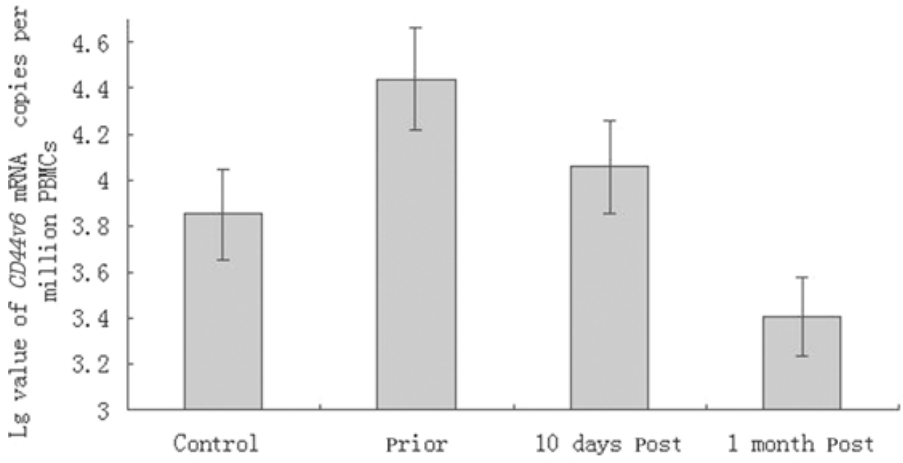

Fig. 5. The levels of *CD44v6* expression in the control group and pancreatic cancer patients prior and post cryotherapy. The expression levels of *CD44v6* in patients prior and 10 days post cryotherapy were significantly higher than that of the control group ($P < 0.05$), whereas no significant difference was found between the patients 1 month post cryotherapy and control ($P > 0.05$). There was no significant difference between the patients prior cryotherapy and 10 days post cryotherapy ($P > 0.05$). *CD44v6* levels in patients 1 month post cryotherapy were significantly decreased compared with the patients prior cryotherapy ($P < 0.05$).

conventional methods. Third, PCR amplification is measured in real-time PCR cycling, so the time of post-PCR analysis is saved and the chances of laboratory contamination by PCR products are reduced because gel electrophoresis procedures are not required.

A one-step SYBR-Green real-time RT-PCR method has also been developed to detect *CD44v6* gene [27]. In this method, the copy number of RNA could not be measured because of difficulty in calculating the length of the nucleotide of RNA, so the concentration of RNA samples was usually measured and was serially diluted to construct the standard curve. However, as the concentration instead of copy number was used to evaluate the gene expression, it cannot reflect the actual gene expression levels. In addition, although the one-step real-time PCR was simple and convenient, RNA template was quite difficult to store because of the degradation, especially during the course of optimizing the reaction system and procedure. Finally, the *CD44v6* and control genes must be detected in different reactions in this one-step real-time PCR, so it was difficult to ensure the consistency of reaction conditions, such as the template content and amplification efficiency; it also produced many errors in the data calculation. In our study, the TaqMan probes used in the duplex qRT-PCR were designed in proximity to the primers and could bind only to specific amplicons. Therefore, the new assay provided further specificity, which was essential for the PCR assay. The recombinant plasmids of *CD44v6* and control genes were constructed successfully and their copy number was calculated by the Dalton equation, which had been widely used to measure the copy number of plasmids in many studies on real-time PCR assay [28],[29]. In this assay, according to the standard curves generated from serially diluted plamids, the copy numbers of *CD44v6* and human β-*actin* genes were measured in a single reaction using the two-step protocol. Moreover, both the reaction efficiency and linear relation in the *CD44v6* and human β-*actin* gene amplification were similar in the duplex qRT-PCR assay after optimization. Thus, this assay could determine the precise gene expression levels with less error compared with a one-step real-time PCR assay. Because of the steady expression for β-*actin* gene in the different tissues or cells, it was able to determine the copy number of *CD44v6* per million host cells using this assay. Therefore, the error in RNA extraction in the different samples could be eliminated and the levels of *CD44v6* expression in different samples or different experimental groups could be compared effectively.

This assay and a conventional RT-PCR assay were used to test the expression levels of *CD44v6* gene in 37 patients with pancreatic cancer. The results confirmed that some samples with very low levels of *CD44v6* expression could not be tested positive by the conventional RT-PCR because of the lack of sensitivity. The study showed that the expression levels of *CD44v6* among male patients were significantly higher than those of female patients ($P < 0.05$), which was consistent with the findings of Chen [30]. This indicates that sex may be one of the possible factors that affect the development of pancreatic cancer. The levels of *CD44v6* expression in the body and tail of the pancreatic cancer were higher than those in the head of pancreatic cancer ($P = 0.068$). This, for the first time, verifies the association between high expression levels of *CD44v6* and the location of tumors. This study found that for patients with tumors larger than 4 cm, with a medium or highly differentiated degree at the intravenous clinical stage, with lymph node or liver metastasis, the levels of *CD44v6* expression were significantly higher than for the patients with tumors smaller than 4 cm, with a low differentiated degree, at the I–III clinical stage, without lymph node or without liver metastasis, respectively ($P < 0.05$), which was consistent with previous studies [31],[32]. This study suggests that *CD44v6* plays an important role in the progression and metastasis of pancreatic cancer and can be used as an important biological marker for predicting the metastatic potential of pancreatic cancer.

In recent years, argon–helium cryosurgery has provided a novel therapeutic approach and has been used for the treatment of tumors, especially for unresectable tumors [33–35]. There are a few reports on cryosurgery for pancreatic cancer [36],[37]. This study confirmed that the expression levels of *CD44v6* in patients prior and 10 days post cryosurgery were significantly higher than in healthy people ($P < 0.05$), proving the association between *CD44v6* and the occurrence and development of pancreatic cancer. In this study, the expression levels of *CD44v6* decreased gradually post cryotherapy, and the expression levels in patients 1 month post cryotherapy were significantly lower than those prior to cryotherapy ($P < 0.05$), showing no significant change compared with the control group ($P > 0.05$). This implies that cryotherapy may possibly play an important role in inhibiting the development and metastasis of pancreatic cancer.

In conclusion, the duplex qRT-PCR assay has been identified as being far more significant than conventional methods to detect the expression levels of *CD44v6* mRNA. *CD44v6* can be regarded as an important biological marker for the evaluation of metastasis and prognosis of pancreatic cancer.

5. Conclusion

We have successfully developed the duplex real-time RT-PCR assay for the detection of *CD44v6* gene in pancreatic cancer patients. This assay was more sensitive and specific compared with conventional methods. Thus, this new method may play a significant role in better understanding the relationship between the expression of *CD44v6* mRNA and the diagnosis, invasion, and metastasis of pancreatic cancer.

Acknowledgements

This work was supported by the Fuda Cancer Hospital of Guangzhou in People's Republic of China and conducted at the Stem Cell Research Group of Guangzhou Institutes of Biomedicine and Health, Chinese Academy of Sciences. We would like to express appreciation to Xiaopeng Liu, Zhiju Zhao, Chengqian Feng, and Mengtian Liao for processing clinical samples.

References

[1] Michalski, C. W., Weitz, J., and Buchler, M. W (2007) *Nat. Clin. Pract. Oncol.* **24**, 526–535.
[2] Jemal, A., Siegel, R., and Ward, E. (2006) *Cancer J. Clin.* **56**, 106–110.
[3] Ryu, J. K., Hong, S. M., and Karikari, C. A. (2010) *Pancreatology* **10**, 66–73.
[4] Rodrigo, J. P., Dominguez, F., and Alvarez, C. (2003) *Am. J. Otolaryngol.* **24**, 384–389.
[5] Lyons, A. J. and Jones, J. (2007) *Int. J. Oral Maxillofac. Surg.* **36**, 671–679.
[6] Gu, H., Ni, C., and Zhan, R. (2000) *Zhonghua Yixue Zazhi* **80**, 854–857.
[7] Weber, G. F., Bronston, R T., and Ilagan, J. (2002) *Cancer Res.* **62**, 2281–2286.
[8] Wang, F. L. and Wei, L. X. (2001) *Zhongguo Yixue Kexueyuan Xuebao* **23**, 401–402.
[9] Yan, R. L., Qian, X. H., and Xin, X. Y. (2002) *Ai. Zheng* **21**, 39–44.
[10] Ylagan, L. R., Scholes, J., and Demopoulos, R. (2000) *Arch. Pathol. Lab. Med.* **124**, 212–215.
[11] Shimabukuro, K., Toyama-Sorimachi, N., and Ozaki, Y. (1997) *Gynecol. Oncol.* **64**, 26–34.
[12] Boxus, M., Letellier, C., and Kerkhofs, P (2005) *Virological Methods* **125**, 125–130.
[13] Shi, X., Lin, L. I., Chen, S. Y., Chao, S. H., Zhang, W., and Meldrum, D. R. (2011) *Laboratory Chip* **5**, 23.
[14] Zhong, L. P., Li, J., and Zhang, C. P. (2007) *Arch. Oral Biol.* **52**, 740–747.
[15] Rodrigo, J. P., Dominguez, F., and Alvarez, C. (2003) *Am. J. Otolaryngol.* **24**, 384–389.
[16] Rautava, J., Soukka, T., and Inki, P. (2003) *Oral Oncol.* **39**, 373–379.
[17] Kanke, M., Fujii, M., and Kameyama, K. (2000) *Arch. Otolaryngol. Head Neck Surg.* **126**, 1217–1223.
[18] Vizoso, F. J., Fernández, J. C., and Corte, M. D. (2004) *J. Cancer Res. Clin. Oncol.* **130**, 679–680.
[19] Yamamichi, K., Uehara, Y., and Kitamura, N. (1998) *Cancer* **79**, 256–262.
[20] Fasano, M., Sabatini, M. T., and Wieczorek, R. (1997) *Cancer* **80**, 34–41.
[21] Klatte, T., Seligson, D. B., and Rao, J. Y. (2010) *J. Urol.* **183**, 2403–2408.
[22] Saito, H., Tsujitani, S., and Katano, K. (1998) *Cancer* **83**, 1094–1098.
[23] Miyoshi, T. and Konda, K. (1997) *Clin. Cancer Res.* **3**, 1289–1292.
[24] Livak, K. J. (2001) *Methods* **5**, 402–408.
[25] Pierga, J. Y. and Bonneton, C. (2005) *Int. J. Cancer* **114**, 291.
[26] Dasif, F., Liedos, G., and Garcia, G. (2001) *Lab. Invest.* **81**, 767–772.
[27] Li, H., Guo, L., and Li, J. (2000) *Oncol.* **17**, 927–932.
[28] Nadya, R., Juan, C., and Nagy, E. (2009) *J. Virol. Methods* **159**, 58–63.
[29] Eeva, K., Michaela, N., and Aimo, A. (2003) *J. Virol. Methods* **112**, 53–65.
[30] Chen, J. (1989) *J. Int. Cancer* **2**, 314–317.
[31] Klatte, T., Seligson, D. B., and Rao, J. Y. (2010) *J. Urol.* **183**, 2403–2408.
[32] Saito, H., Tsujitani, S., and Katano, K. (1998) *Cancer* **83**, 1094–1098.
[33] Xu, K. C. and Niu, L. Z. (2003) *World J. Gastroenterol.* **59**, 2686–2689.
[34] Mouraviev, V. and Polascik, T. J. (2006) *Curr. Opin. Urol.* **16**, 152–156.
[35] Xu, K. C. and Niu, L. Z. (2003) *World J. Gastroenterol.* **9**, 2688–2689.
[36] Kovach, S. J. and Hendrickson, R. J. (2003) *Surgery* **131**, 463–465.
[37] Korpan, N. N. (2001). Pancreas cryosurgery, In Basics of Cryosurgery (Korpan, N. N., ed.). 1st ed. Springer-Verlag, Weinham, Germany.